Bioresource Technology 166 (2014) 389–394

Contents lists available at ScienceDirect

Bioresource Technology

journal homepage: www.elsevier.com/locate/biortech

Comparison of membrane foulants occurred under different sub-critical flux conditions in a membrane bioreactor (MBR)

Tran-Ngoc-Phu Nguyen [a], Yu-Chun Su [b], Jill Ruhsing Pan [c], Chihpin Huang [a,*]

[a] Institute of Environmental Engineering, National Chiao Tung University, Hsinchu 300, Taiwan
[b] Disaster Prevention and Water Research Center, National Chiao Tung University, Hsinchu 300, Taiwan
[c] Department of Biological Science and Technology, National Chiao Tung University, Hsinchu 300, Taiwan

HIGHLIGHTS

- A higher fouling propensity was caused by the soluble proteins and polysaccharides.
- The cell-bound proteins and polysaccharides were dominant in hydrophobic membrane.
- Proteins and polysaccharides were mostly in the middle of the cake layer thickness.

ARTICLE INFO

Article history:
Received 26 February 2014
Received in revised form 19 May 2014
Accepted 21 May 2014
Available online 28 May 2014

Keywords:
Extracellular polymeric substances
Membrane bioreactor
Membrane foulants
Sub-critical flux

ABSTRACT

Membrane fouling precludes the widespread application of membrane filtration system from treating wastewater and drinking water, and occurs even under sub-critical flux operations. Hence the characteristics and behavior of membrane foulants should be thoroughly investigated, so as to find ways to reduce membrane fouling in membrane bioreactors. The purpose of this study is to compare the membrane fouling potential at different sub-critical flux operations and for different hydrophobic/hydrophilic membranes, and to investigate the vertical distribution of membrane foulants in a cake layer. Results showed that higher fouling propensity which occurred under 80% of critical flux of hydrophilic membrane was associated with the soluble fraction of proteins and polysaccharides, compared with 60% of critical flux. The cell-bound components were dominant under hydrophobic membrane operation. The highest concentration of proteins and polysaccharides was found between 40% and 80% of the depth of the cake layer.

1. Introduction

In recent years, membrane filtration technologies have become more and more popular in water reclamation as well as in wastewater treatment. MBR, which combines membrane filtration and biodegradation, is a particular method for treating wastewater. However, membrane fouling during use, which increases operational and material costs, has been considered a major obstacle to the extensive use of MBRs. Minimizing membrane fouling has thus become a top priority for most researchers interested in MBRs.

Several authors have reported that efficient operation of MBR is dependent on many factors, such as mixed liquor suspended concentration (Trussell et al., 2007), aeration regime (Le-Clech et al., 2003b), sludge retention time (Ng et al., 2013), membrane characteristics (Choi and Ng, 2008), as examples. Membrane characteristics, such as pore size, hydrophobicity, and membrane morphology, also affect membrane fouling propensity as a result of the interaction between membrane and solutes (Le-Clech et al., 2003b; Maximous et al., 2009). Boussu et al. (2007) suggested that using a hydrophilic membrane may minimize fouling tendency. Nevertheless, Maximous et al. (2009) reported on the advantages of using hydrophobic membrane in rejecting polysaccharides and proteins compared with hydrophilic membrane. Further investigation should be carried out to clarify such controversial results.

The critical flux concept was proposed in the middle 1990s (Field et al., 1995). Theoretically, when an MBR system operates at a flux below the critical flux (i.e. sub-critical flux), its permeate flux remains constant. In other words, foulants should not occur in sub-critical flux operation. However, some work has shown that a dramatic increase in fouling rate does occur after operating under sub-critical flux operation for some time (Cho and Fane, 2002). A number of critical flux determination methods have been

* Corresponding author. Tel.: +886 3 5712121x55507; fax: +886 3 5725958.
E-mail address: cphuang@mail.nctu.edu.tw (C. Huang).

http://dx.doi.org/10.1016/j.biortech.2014.05.073
0960-8524/

proposed, such as the flux-step method (Le-Clech et al., 2003b), mass balance technique combined with direct observation image analysis (Zhang et al., 2010), dynamic filtration (Loderer et al., 2013). Among these, the flux-step method combined with 90% permeability ($K > 0.9K_0$) definition can be effectively used in membrane process (Le-Clech et al., 2003b; Tiranuntakul et al., 2011). The flux-step method was then developed to determine the critical flux in an MBR (Le-Clech et al., 2003a), their results showed that step length and height are two important parameters measured by the flux-step method, in which the best choice of step length and step height lie in 15–30 min and 3 l m^{-2} h^{-1}, respectively. The concept of permeability (K, l m^{-2} h^{-1} kPa^{-1}) has also been proposed to accurately verify critical flux. K was plotted against flux to determine critical flux (Le-Clech et al., 2003a). The parameter (K) is obtained as below:

$$K = \frac{J}{P_{ave}} \quad (1)$$

$$P_{ave} = \frac{TMP_f^n + TMP_i^n}{2} \quad (2)$$

where TMP_i^n and TMP_f^n are the initial and final transmembrane pressures (TMP) (kPa), respectively. J is the arbitrary permeate flux (l m^{-2} h^{-1}), and t_i^n, t_f^n are the initial and final point time of each step length, respectively. P_{ave} is the average pressure of each step length (kPa).

In an earlier study, Le-Clech et al. (2006) classified membrane foulants into standard blocking, intermediate blocking, complete blocking or cake filtration. Several authors reported that the cake layer contributed up to 80% of total resistance, and is the dominant foulant (Maximous et al., 2009; Qu et al., 2014; Lee et al., 2001). Moreover, extracellular polymeric substances (EPS) were found to be one of the main components of cake layer (Cho and Fane, 2002; Wang et al., 2009; Wu and Lee, 2011), and identified as the complex high-molecular weight mixtures of polymers in biomass such as activated sludge and biofilm produced from metabolism or the cell lysis processes. The major components of EPS include polysaccharides, proteins, nucleic acids, and lipids (Sheng et al., 2010). In several studies, polysaccharides were considered the main components of EPS, while proteins were much less so, or were below detection limits (Pan et al., 2010; Drovak et al., 2011). Li et al. (2013) found that membrane fouling took place under sub-critical flux conditions in three stages, in which cell-bound fractions play an important role in the first stage, after which soluble fractions accelerate final blocking of the membrane pores.

To examine the structure of microbial cells and biofilm, confocal laser scanning microscopy (CLSM) has been widely used in MBRs (Chen et al., 2006; Hwang et al., 2012). Chen et al. (2006) reported that foulant components such as proteins and polysaccharides can be simultaneously detected via CLSM by using a quadruple staining method. Ng and Ng (2011) also used CLSM to identify that the fouling mechanisms changed from a biofilm predominantly attached to polyolefin membranes, to a bio-organic layer on polyethersulfone membrane under sub-critical flux operation. Although many studies have been focused on membrane fouling under sub-critical flux operation, little information is available on the compositions of foulants, as well as on their distribution in a cake layer. Further research is thus necessary in order to provide a correlation between membrane foulants composition and membrane hydrophobicity under different sub-critical flux conditions. The aim of this study was: (1) to compare the fouling potential under two different sub-critical flux conditions using a hydrophilic membrane; (2) to evaluate the correlation between hydrophilic/hydrophobic membranes and membrane fouling under sub-critical flux operation, and (3) to investigate the vertical distribution of foulants in the cake layer.

2. Methods

2.1. Experimental setup

A 30-L MBR was used in this study, the detailed information of which is given in Pan et al. (2010). Synthetic wastewater was prepared as influent as in Ng and Hermanowicz (2005). Hydrophilic (HPI) and hydrophobic (HPO) flat-sheet membranes (King Membrane Company, Taiwan) were used. The membranes are made of polytetrafluoroethylene (PTFE) with mean pore size of 0.5 μm and total surface area of 0.1 m^2. The contact angle of the membranes was 65° and 120° for HPI and HPO membranes, respectively. In order to keep a constant flux operation, an automatic control system was designed by ADAMview software. When the system was operating, the flow-rate signal was transferred from the flow meter to the computer and the pump speed was controlled to adjust the flow-rate as constant as computed. Feed solution was stored in a refrigerator, and was continuously pumped into the bioreactors from a 60-L feed solution tank. Tap water was supplied to maintain the water level and was controlled by a float switch. The average total organic carbon of MBR influent was 160 ± 10 mg l^{-1}. To control the pH at 6.5–7.5, hydrochloric acid was automatically added into the MBR if needed. Air was also continuously supplied from the bottom of the tank through air diffusers below the membrane modules to keep the dissolved oxygen at $\geqslant$2 mg l^{-1}. Sludge retention time (SRT) was set at 10 days. The mixed liquor suspended solids (MLSS) concentration was stable in the range of 6000–6500 mg l^{-1}.

2.2. Flux-step method for determining critical flux

The flux-step method was applied to determine critical flux. Initial flux was selected at 6 l m^{-2} h^{-1}, and operational fluxes were varied between 6 and 45 l m^{-2} h^{-1} with a step height of 3 l m^{-2} h^{-1} and step length of 15 min. The changes of TMP were automatically recorded by the computer. Critical flux is defined as the flux at which $K > 0.9K_0$, where K_0 (l m^{-2} h^{-1} kPa^{-1}) is the initial permeability measured from the first flux-step (Le-Clech et al., 2003b; Guglielmi et al., 2007). K and K_0 were calculated by using Eqs. (1) and (2).

2.3. Analytical methods

2.3.1. Membrane foulants collection

As soon as the TMP reached about −40 kPa, the flat-sheet membrane was removed from the MBR. The cake layer surface was then washed softly with deionized water. All the foulants on one side of the membrane sheet (0.05 m^2) were then scraped off with a hard plastic sheet. Next, the collected foulants were placed in a beaker with 75 ml deionized water and well mixed with a magnetic stirrer. The foulants taken from the cake layer was then analyzed.

2.3.2. Extraction of EPS

As noted above, the main composition of EPS is considered as proteins and polysaccharides. Further, EPS has been demonstrated by many investigators that it is the most important membrane foulant. In order then to characterize membrane foulants, EPS should be much more concentrated. EPS thus has to be separated from the other membrane foulants so as to determine its composition. Different EPS extraction methods have been proposed: thermal treatment (Wang et al., 2009) and formaldehyde-NaOH extraction (Liu and Fang, 2002). In this study, we selected the formaldehyde-NaOH extraction method, because of the advantages demonstrated by Liu and Fang (2002).

First, 10 ml sludge was centrifuged (U-320R Boeco, Germany) at 4000 rpm, and 4 °C for 20 min to separate the sludge from the

liquid. The liquid was filtered through 0.45 μm membrane to obtain soluble EPS. 10 ml deionized water was used to re-suspend the solids. Then, 0.06 ml 36.5% formaldehyde was added into the suspension and kept at 4 °C for 60 min in order to fix the cells to prevent lysis. Next, 4 ml of 1 N NaOH was added into the suspension to increase pH, resulting in the dissociation of acidic groups in the EPS. The suspension was then refrigerated at 4 °C for 180 min. The suspension then was centrifuged at 20,000*g* at 4 °C for 20 min and filtrated through a 0.2 μm membrane to remove the microbial cells. Bound EPS was obtained after purification with a 3500 Da dialysis membrane at 4 °C for 2 days to remove the extractant residues in the solution.

2.3.3. Determination of polysaccharides in membrane foulants

Polysaccharides were quantified by the phenol–sulfuric acid method, which was first established by Dubois et al. (1956). 1 ml 5% phenol was added to 1 ml of filtrate, which separates most of sugars in the sample. Next, 5 ml of 75% sulfuric acid was added to the mixture for 10 min to remove the residual phenol, and the tube was then stood in water bath at 25 °C for 15 min for complete reaction. After the complete reaction, the absorbance of the samples was then measured at a wavelength of 488 nm. The calibration curve was obtained by plotting the absorbance versus the glucose concentration of 5, 10, 20, 40, and 80 mg l^{-1}.

2.3.4. Determination of proteins in membrane foulants

To determine the concentration of proteins, the Bradford method (1976) was used. 3 ml of Bradford reagent (Sigma–Aldrich) was added to 0.1 ml of sample, and then rapidly mixed at ambient temperature for 5–45 min. The absorbance of the samples was then measured at a wavelength of 595 nm. To plot the calibration curve, Bovine Serum Albumin (BSA) was used as the protein standard with a concentration range of 0.1–1 mg ml^{-1}. Where protein concentration was less than 0.1 mg ml^{-1}, the procedure was slightly modified as per the manual provided by Sigma–Aldrich, and the protein concentration was changed to a range of 1–10 μg ml^{-1} in the calibration curve.

2.3.5. Identification of foulants

A CLSM (Leica TCS SP2 Confocal Spectral Microscope Image System, Germany) was used to determine the compositions of the membrane foulants. Three fractions of membrane were randomly taken from the membrane module after being removed from reactor for staining when the TMP reached about −40 kPa. Besides, a blank sample (clean membrane) stained with the same procedure was prepared for collating. Fluorescein isothiocyanate (FITC) (Molecular Probes, USA), Concanavalin A (ConA) (Molecular Probes, USA) and Fluorescent Brightener 28 (Calcoflour white, CW) (Sigma) were used to stain the proteins, α-D-glucopyranose polysaccharides and β-D-glucopyranose polysaccharides, respectively. Staining were followed the procedure described by Chen et al. (2006). Proteins were detected via excitation at 488 nm and emission wavelengths of 500–550 nm. To detect α-D-glucopyranose polysaccharides, excitation wavelength of 543 nm and emission range of 550–590 nm was applied. The presence of β-D-glucopyranose polysaccharides were determined via excitation at 400 nm and emission at 410–418 nm.

3. Results and discussion

3.1. Critical flux assessment and different sub-critical flux operations

In order to carry out this study, critical flux was first measured based on the permeability as described in Section 2.2. The permeability values for HPI and HPO membranes are given in Table 1. For HPI membrane, the initial permeability (K_0) was 21.8 l m^{-2} h^{-1} - kPa^{-1}, and therefore $0.9K_0$ was 19.62 l m^{-2} h^{-1} kPa^{-1}. Based on the $K > 0.9K_0$, critical flux was 33 l m^{-2} h^{-1}. Two different sub-critical fluxes at 60% and 80% of critical flux (i.e. 19.8 l m^{-2} h^{-1} and 26.4 l m^{-2} h^{-1}, respectively) were then operated to compare the fouling potential under different sub-critical flux conditions, and are given as 60% (HPI) and 80% (HPI), respectively. Similarly, critical flux of HPO membrane was 30 l m^{-2} h^{-1} and 80% of critical flux (i.e. 24 l m^{-2} h^{-1}) which is given as 80% (HPO) was operated thereafter.

Table 1
Permeability and fouling rate in flux-step experiment.

Flux (l m^{-2} h^{-1})	Permeability (l m^{-2} h^{-1} kPa^{-1})		Flux (l m^{-2} h^{-1})	Permeability (l m^{-2} h^{-1} kPa^{-1})	
	HPI	HPO		HPI	HPO
6	21.8	24.6	27	23.7	23.7
9	22.2	26.1	30	22.2	22.3
12	26.4	23.7	33	20.2	21.0
15	22.5	24.1	36	19.2	19.0
18	22.7	23.4	39	19.5	17.1
21	23.2	23.3	42	19.6	15.5
24	24.7	23.5	45	18.8	12.9

Fig. 1 shows the variation of TMP with operation time under different sub-critical fluxes with hydrophobic/hydrophilic membranes. For the first 6 days of operation, the TMP changes of these three runs were almost similar with a slight increase from nearly 0 to approximately −7 kPa. The increase of TMP indicates the deposition of membrane foulants even under sub-critical flux (Cho and Fane, 2002). The TMP jump occurred after about 7-days operation for 80% (HPO), while it took about 12-days for both 80% (HPI) and 60% (HPI). After operating for 6 days, the TMP of 80% (HPI) began to exceed that of 60% (HPI) until 15 days, and the TMP tended to be similar again.

The profiles of TMP changes for all runs in this study are consistent with the hypothesis of two-stage process of membrane fouling formed under sub-critical flux operation proposed by Cho and Fane (2002). The deposition of EPS was the main reason causing the gradual increase of TMP for all runs in the first 6 days of operation (Cho and Fane, 2002). Zhang et al. (2006) suggested that the reason for this phenomenon is caused by biopolymer deposition and biofilm formation. The sudden increase in TMP occurred in all runs at a specific operational time as a result of the deposition of a large amount of polysaccharides excreted by biomass activities (Zhang et al., 2006). The faster TMP jump of 80% (HPO) compared with 80% (HPI) can be explained by considering the hydrophobic-hydrophobic interaction of solutes and membranes (Jarusutthirak et al., 2002). In other words, the foulants attach more easily to a hydrophobic membrane surface than a hydrophilic one, resulting the higher fouling propensity of HPO membrane. It was very obviously that the higher TMP was observed from 80% (HPI) compared with 60% (HPI) because of the higher suction force applied. The plateau in TMP at the tenth day of 80% (HPI) might be attributed to the reversible attachment of foulants on membrane surface. In other words, the shear stress could not detach the removable foulants until TMP reached the peak of −16 kPa, resulting in the abnormal increase in TMP. Eventually, the cake layer covered the membrane surface for all runs and kept TMP stably increasing after TMP reached approximately −35 kPa.

3.2. Membrane foulant composition under different sub-critical flux operations

Proteins and polysaccharides, the main components of EPS, are foulants in an MBR (Zhang et al., 2006), and are generated by the activities of microorganisms. To identify the compounds in a cake

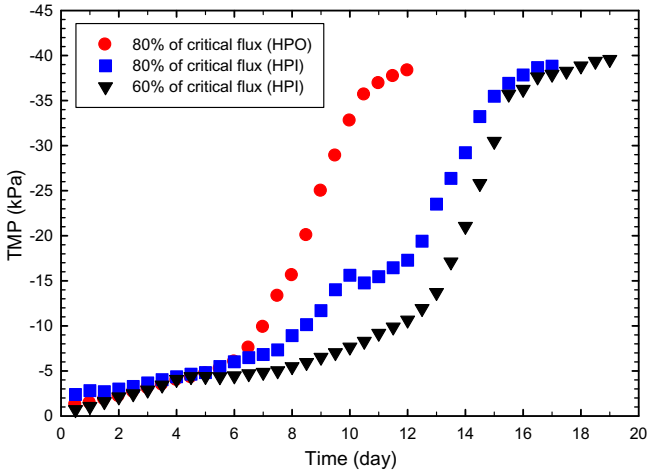

Fig. 1. Long-term TMP change under different sub-critical flux with hydrophobic/hydrophilic membranes.

layer, a Fourier Transform Infrared (FTIR) spectrophotometer was used. Proteins and polysaccharides were detected on both types of membrane confirming then as dominant components of membrane foulants (see Appendix A.1).

Because proteins and polysaccharides are main compositions of membrane foulants, they are mentioned by many authors in order to investigate the impact of fouling against the membrane (Pan et al., 2010; Ng and Ng, 2010), and this was confirmed by this study. The soluble and cell-bound fractions of proteins and polysaccharides in cake layer under different operational conditions are shown in Fig. 2. Fig. 2a shows that the concentration of soluble polysaccharides of 80% (HPI) (101.34 ± 44.31 mg l^{-1} as glucose) was much higher than that of 60% (HPI) (31.34 ± 5.88 mg l^{-1} as glucose). On the other hand, 60% (HPI) had slightly higher cell-bound polysaccharides concentration (35.14 ± 0.19 mg g^{-1} MLSS as glucose) than that of 80% (HPI) (27.83 ± 5.46 mg g^{-1} MLSS as glucose). These results show that the different fouling rates found may mainly result from the significant difference of soluble polysaccharides in the cake layer. In other words, the higher concentration of soluble polysaccharides of 80% (HPI) resulted in the higher TMP increase than 60% (HPI). Pan et al. (2010) found that high concentration of soluble polysaccharides caused extreme fouling in MBR. In the case of 80% (HPO), the concentration of soluble polysaccharides (12.96 ± 0.26 mg l^{-1} as glucose) was considerably lower than that of 80% (HPI), while the cell-bound polysaccharides concentration (61.21 ± 1.9 mg g^{-1} MLSS as glucose) was slightly more than twice as high. Furthermore, a rapid increase of TMP was observed at 80% (HPO), and we conclude that the higher TMP increase of 80% (HPO) may be caused by cell-bound polysaccharides, compared to 80% (HPI). Ng and Ng (2010) reported that proteins on membrane fouling are crucial in MBRs under different flux conditions, and Fig. 2b shows the concentration of soluble and cell-bound proteins in the cake layer. The concentration of soluble proteins of 80% (HPI) (36.25 ± 6.29 mg l^{-1} as BSA) was higher than that of 60% (HPI) (9.51 ± 0.19 mg l^{-1} as BSA) while the cell-bound proteins of 80% (HPI) (21.09 ± 1.27 mg g^{-1} MLSS as BSA) was much lower than that of 80% (HPO) (262.26 ± 3.52 mg g^{-1} MLSS as BSA).

In summary, as can be seen from the Fig. 2, the soluble fraction of proteins and polysaccharides resulted in the higher fouling propensity of 80% (HPI) (36.25 ± 6.29 mg l^{-1} as BSA and 101.34 ± 44.31 mg l^{-1} as glucose) compared with 60% (HPI) (9.51 ± 0.19 mg l^{-1} as BSA and 31.34 ± 5.88 mg l^{-1} as glucose) while cell-bound fraction of those related to the higher fouling potential of 80% (HPO) (262.26 ± 3.52 mg g^{-1} MLSS as BSA and 61.21 ± 1.9 mg g^{-1} MLSS as glucose) compared with 80% (HPI) (21.09 ± 1.27 mg g^{-1} MLSS as BSA and 27.83 ± 5.46 mg g^{-1} MLSS as glucose).

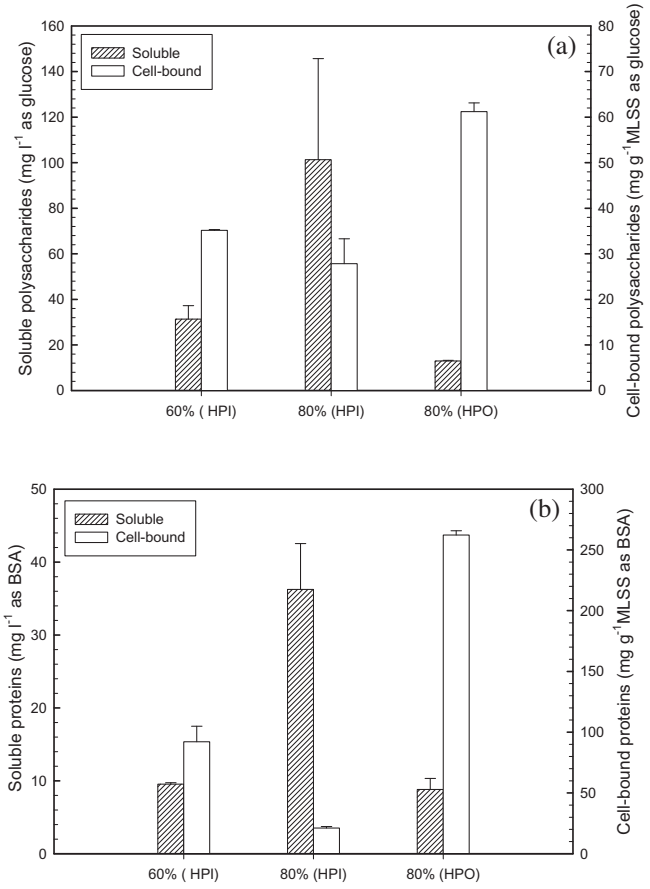

Fig. 2. Polysaccharides and proteins of membrane foulants in cake layer (a) polysaccharides; (b) proteins.

3.3. Distribution of fouling compositions in foulants

Proteins and polysaccharides in membrane foulants can be directly observed using CLSM technology. Three confocal scan positions on three different samples were examined to obtain statistics. In CLSM images, proteins, α-D-glucopyranose polysaccharides, and β-D-glucopyranose polysaccharides are shown in green, cyan, and blue, respectively (detailed in Appendix A.2). These images also confirm that proteins and α-D-glucopyranose polysaccharides as the main contributors to membrane fouling, while the effect of β-D-glucopyranose polysaccharides was insignificant. To gain a better understanding of cake layer composition, the vertical distribution of these compounds was next investigated.

The thickness of cake layers was 62.4 ± 3.89 μm, 102.57 ± 5.37 μm, and 76.93 ± 4.88 μm for 60% (HPI), 80% (HPI), and 80% (HPO), respectively. The mechanism of deposition of particles on membrane surface is very complicated because of the complex composition of sludge, operating dynamics, as well as the interaction between solutes and membrane, and as a result the distribution of the components in a cake layer is uneven (Zhang et al., 2006), and the cake layer thickness differs at different places on the membrane. To compare the relative vertical distribution of foulants in cake layers, the intensities of the fluorescent lights probed at specific position above membrane. In other words, the cake was cut at 9 points and marked from 0 to 1 at each cutting point corresponding to from 0% to 100% of the cake layer thickness.

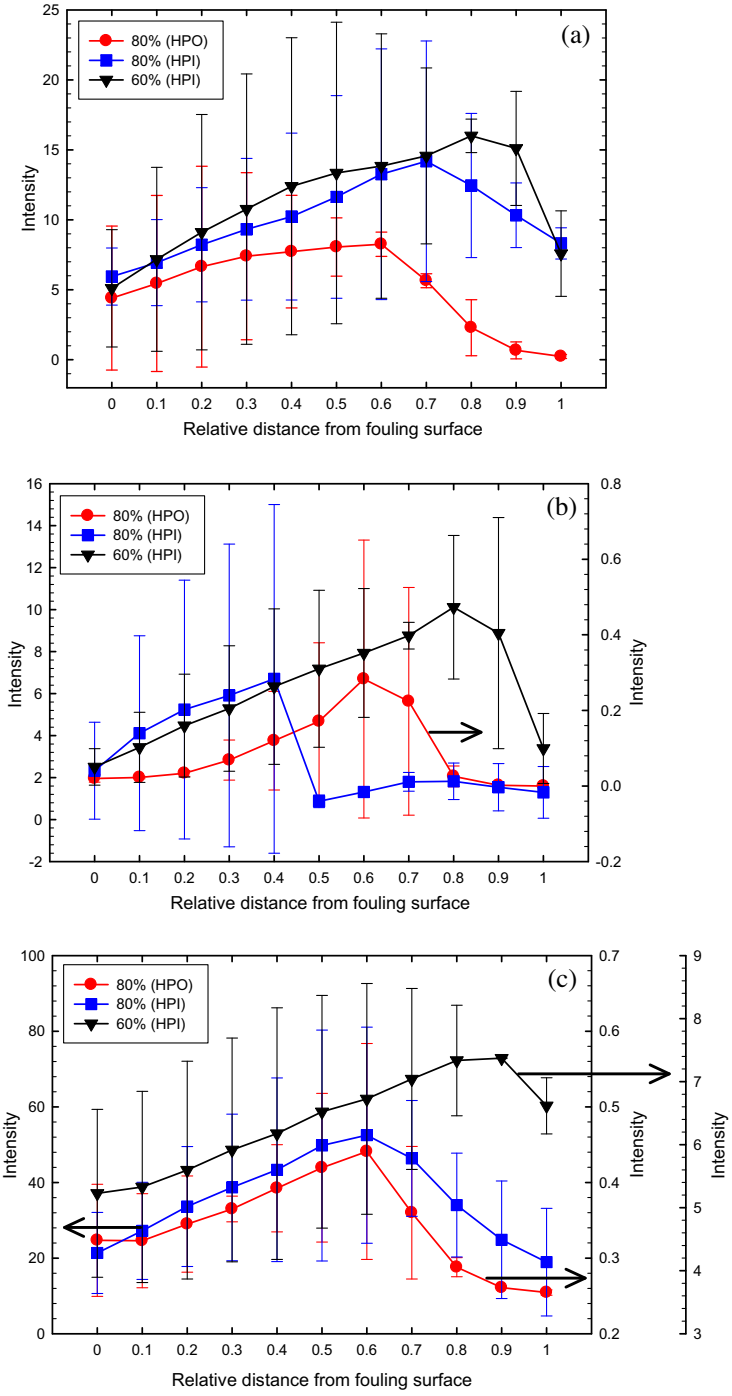

Fig. 3. Vertical distribution of proteins and polysaccharides from the surface of cake layer to the membrane surface: (a) protein; (b) α-D-glucopyranose polysaccharides; (c) β-D-glucopyranose polysaccharides.

Fig. 3 shows the vertical distribution of proteins, α-D-glucopyranose polysaccharides, and β-D-glucopyranose polysaccharides.

At the initially deposited layer, nearest membrane surface (position 1), the intensities of the fluorescent lights corresponding to proteins, α-D-glucopyranose polysaccharides, and β-D-glucopyranose polysaccharides were relatively low. The intensities then increased with the increase of cake layer thickness. The deposition of proteins through the cake depth of 60% (HPI), 80% (HPI), and 80% (HPO) are shown in Fig. 3a. The low protein concentration at the beginning of the cake layer might be explained by the attachment of inorganic and non EPS substances on the membrane surface to form the first layer. Allison and Sutherland (1987) showed that non-polysaccharides were not present at the initial attachment stage, but only after the initial layer had been formed, did microorganisms gradually colonize, grow and then develop a biofilm which became part of cake layer. As a result of the growth of microorganisms on the membrane surface, EPS was released and became the dominant foulant, leading the increase of proteins in the cake layer. As can be seen from Fig. 3a, the peaks for proteins for all runs were at 0.9, 0.8 and 0.6 of the relative distance for 60% (HPI), 80% (HPI) and 80% (HPO), respectively. Another reason for the change of protein concentration in cake layer could be a result of the pressure of the long-term operation. Because of the pressure applied, particles such as colloids, solutes and bacteria cells in sludge solution

gradually accumulates and becomes compressed, causing the dense layer near the membrane surface. This dense layer contained more protein concentration than other levels of the cake layer, resulting the concentration peaks in the middle regions of the cake layer. A similar phenomenon was found for α-D-glucopyranose polysaccharides and β-D-glucopyranose polysaccharides (Fig. 3b and c), where they were mainly found in the middle of the cake layer.

Interestingly, the peaks for proteins, α-D-glucopyranose polysaccharides and β-D-glucopyranose polysaccharides of 60% (HPI) were observed at 80% of depth of cake layer (described by 0.8 of *X*-axis) while the peaks for proteins, α-D-glucopyranose polysaccharides, and β-D-glucopyranose polysaccharides of 80% (HPI) were seen at 0.7, 0.4, and 0.6, respectively. Furthermore, the TMP increase of 80% (HPI) was higher than 60% (HPI) for the period of operation from day 6 to day 15. This indicates that for a lower flux imposed, foulants seems to become more densely compressed than a higher flux. In other words, small particles gradually attach on the membrane surface first and larger particles are then deposited later, whereas at a higher flux, large particles could be forced to become attached and will prevent the formation of a dense layer, with the result that the peaks occurred further from the membrane surface. In the case of 80% (HPO), the peaks for proteins, α-D-glucopyranose polysaccharides, and β-D-glucopyranose polysaccharides were found at 0.6. Although the peaks of these substances could be found at the positions similar to those of 80% (HPI), the TMP increase of 80% (HPO) was faster than that of 80% (HPI). This difference may be a result of the hydrophobic/hydrophilic characteristics of membranes. Qu et al. (2014) reported that hydrophobic membrane is more attractive of adsorptive fouling than hydrophilic membrane, leading to a higher TMP.

4. Conclusions

This study shows that soluble fractions of EPS (mainly proteins and polysaccharides) dominate membrane fouling in an MBR operated at higher sub-critical flux. On the other hand, cell-bound fractions of EPS of hydrophobic membrane contribute to greater membrane fouling and TMP increases compared to hydrophilic membrane. Moreover, the vertical distributions of proteins and polysaccharides fluctuate with the cake layer depth at which proteins and polysaccharides mainly accumulate.

Acknowledgement

The financial support of this work by the National Science Council of the Republic of China (Grant No. 96-2628-E-009-006-MY3) is gratefully acknowledged.

Appendix A. Supplementary data

Supplementary data associated with this article can be found, in the online version, at http://dx.doi.org/10.1016/j.biortech.2014.05.073.

References

Allison, D.G., Sutherland, I.W., 1987. The role of exopolysaccharides in adhesion of freshwater bacteria. J. Gen. Microbiol. 133, 1319–1327.
Boussu, K., Belpaire, A., Bolodin, A., Van Haesendonck, C., Van de Meeren, P., Vandecasteele, C., Van de Bruggen, B., 2007. Influence of membrane and colloid characteristics on fouling of nanofiltration membrane. J. Membr. Sci. 289, 220–230.
Bradford, M.M., 1976. A rapid and sensitive method for the quantitation of microgram quantities of protein utilizing the principle of protein–dye binding. Anal. Biochem. 72, 248–254.
Chen, M.Y., Lee, D.J., Yang, Z., Peng, X.F., Lai, J.Y., 2006. Fluorescent staining for study of extracellular polymeric substances in membrane biofouling layers. Environ. Sci. Technol. 40, 6642–6646.
Cho, B.D., Fane, A.G., 2002. Fouling transients in nominally sub-critical flux operation of a membrane bioreactor. J. Membr. Sci. 209, 391–403.
Choi, J.H., Ng, H.Y., 2008. Effect of membrane type and material on performance of a submerged membrane bioreactor. Chemosphere 71, 853–859.
Drovak, L., Gomez, M., Drovakova, M., Ruzickova, I., Wanner, J., 2011. The impact of different operating conditions on membrane fouling and EPS production. Bioresour. Technol. 102, 6870–6875.
Dubois, M., Gilles, K.A., Hamilton, J.K., Rebers, P.A., Smith, F., 1956. Colorimetric method for determination of sugars and related substances. Anal. Chem. 28, 350–356.
Field, R.W., Wu, D., Howell, J.A., Gupta, B.B., 1995. Critical flux concept for microfiltration fouling. J. Membr. Sci. 100, 259–272.
Guglielmi, G., Chiarani, D., Judd, S.J., Andreottola, G., 2007. Flux criticality and sustainability in a hollow fibre submerged membrane bioreactor for municipal wastewater treatment. J. Membr. Sci. 289, 241–248.
Hwang, B.K., Lee, C.H., Chang, I.S., Drews, A., Field, R., 2012. Membrane bioreactor: TMP rise and characterization of bio-cake structure using CLSM-image analysis. J. Membr. Sci. 419–420, 33–41.
Jarusutthirak, C., Amy, G., Croué, J.P., 2002. Fouling characteristics of wastewater effluent organic matter (EfOM) isolates on NF and UF membrane. Desalination 145, 247–255.
Le-Clech, P., Chen, V., Fane, A.G., 2006. Fouling in membrane bioreactors used in wastewater treatment. J. Membr. Sci. 284, 17–53.
Le-Clech, P., Jefferson, B., Chang, I.S., Judd, S.J., 2003a. Critical flux determination by the flux-step method in a submerged membrane bioreactor. J. Membr. Sci. 227, 81–93.
Le-Clech, P., Jefferson, B., Judd, S.J., 2003b. Impact of aeration, solids concentration and membrane characteristics on the hydraulic performance of a membrane bioreactor. J. Membr. Sci. 218, 117–129.
Lee, J., Ahn, W.Y., Lee, C.H., 2001. Comparison of the filtration characteristics between attached and suspended growth microorganisms in submerged membrane bioreactor. Water Res. 35, 2435–2445.
Li, J.F., Zhang, X.X., Cheng, F.Q., Liu, Y., 2013. New insights into membrane fouling in submerged MBR under sub-critical flux condition. Bioresour. Technol. 137, 404–408.
Liu, H., Fang, H.P., 2002. Extraction of extracellular polymeric substances (EPS) of sludge. J. Biotechnol. 95, 249–256.
Loderer, C., Gahlitner, B., Steinbacher, K., Stelzer, C., Fuchs, W., 2013. Dynamic filtration – a novel approach for critical flux determination using different textiles. Sep. Purif. Technol. 120, 410–414.
Maximous, N., Nakhla, G., Wan, M., 2009. Comparative assessment of hydrophobic and hydrophilic membrane fouling in wastewater applications. J. Membr. Sci. 339, 93–99.
Ng, C.A., Sun, D., Bashir, M.J.K., Wai, S.H., Wong, L.Y., Nisar, H., Wu, B., Fane, A.G., 2013. Optimization of membrane bioreactors by the addition of powdered activated sludge. Bioresour. Technol. 138, 38–47.
Ng, T.C.A., Ng, H.Y., 2010. Characterisation of initial fouling in aerobic submerged membrane bioreactors in relation to physico-chemical characteristics under different flux conditions. Water Res. 44, 2336–2348.
Ng, T.C.A., Ng, H.Y., 2011. Physico-chemical characterisation versus in situ microstructural characterisation of membrane fouling in membrane bioreactors. Water Sci. Technol. 63, 1781–1787.
Ng, Y.H., Hermanowicz, S.W., 2005. Membrane bioreactor operation at short retention times: performance and biomass characteristics. Water Res. 39 (6), 981–992.
Pan, J.R., Su, Y.C., Huang, C.P., Lee, H.C., 2010. Effect of sludge characteristics on membrane fouling in membrane bioreactors. J. Membr. Sci. 349, 287–294.
Qu, F.S., Liang, H., Zhou, J., Nan, J., Shao, S.L., Zhang, J.Q., Li, G.B., 2014. Ultrafiltration membrane fouling caused by extracellular organic matter (EOM) from *Microcystis aeruginosa*: effects of membrane pore size and surface hydrophobicity. J. Membr. Sci. 449, 58–66.
Sheng, G.P., Yu, H.Q., Li, X.Y., 2010. Extracellular polymeric substances (EPS) of microbial aggregates in biological wastewater treatment systems: a review. Biotechnol. Adv. 28, 882–894.
Tiranuntakul, M., Schneider, P.A., Jegatheesan, V., 2011. Assessments of critical flux in a pilot-scale membrane bioreactor. Bioresour. Technol. 102, 5370–5374.
Trussell, R.S., Merlo, R.P., Hermanowicz, S.W., Jenkins, D., 2007. Influence of mixed liquor properties and aeration intensity on membrane fouling in a submerged membrane bioreactor at high mixed liquor suspended solids concentrations. Water Res. 41 (5), 947–958.
Wang, Z.W., Wu, Z.C., Tang, S.J., 2009. Extracellular polymeric substances (EPS) properties and their effects on membrane fouling in a submerged membrane bioreactor. Water Res. 43, 2504–2512.
Wu, S.C., Lee, C.M., 2011. Correlation between fouling propensity of soluble extracellular polymeric substances and sludge metabolic activity altered by different starvation conditions. Bioresour. Technol. 102, 5375–5380.
Zhang, J., Chua, H.C., Zhou, J., Fane, A.G., 2006. Factors affecting the membrane performance in submerged membrane bioreactors. J. Membr. Sci. 284, 54–66.
Zhang, Y.P., Lawa, A.W.K., Fane, A.G., 2010. Determination of critical flux by mass balance technique combined with direct observation image analysis. J. Membr. Sci. 365, 106–113.